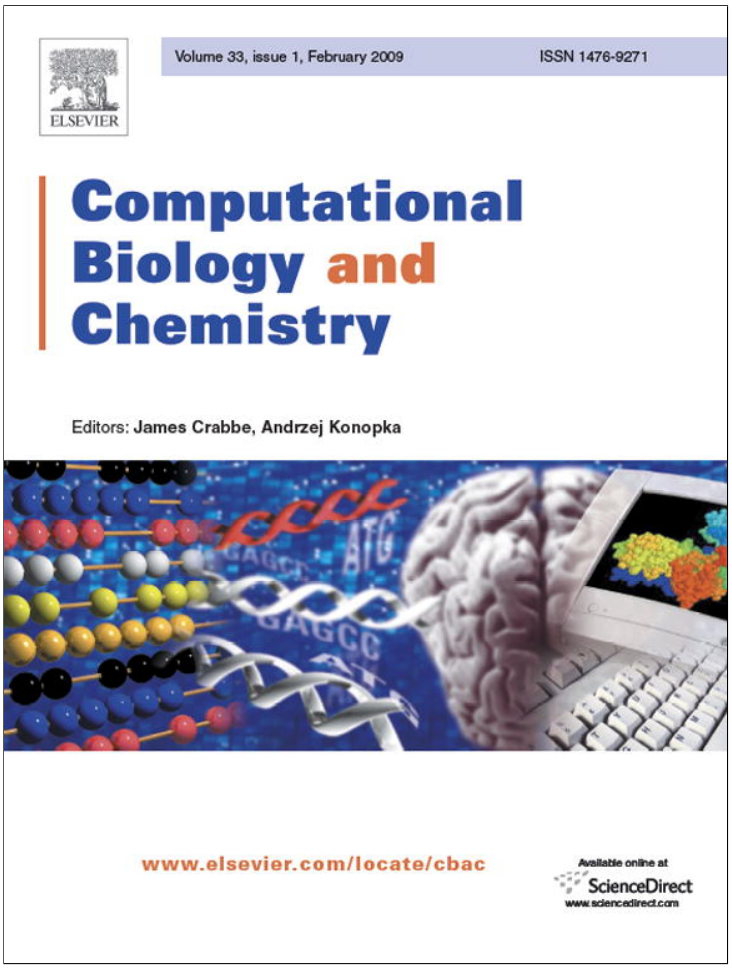

Computational Biology and Chemistry 33 (2009) 33–40

Contents lists available at ScienceDirect

Computational Biology and Chemistry

journal homepage: www.elsevier.com/locate/compbiolchem

Research Article

Mathematical modelling of NABD release from endoluminal gel paved stent

L. Davia[a], G. Grassi[b,c], G. Pontrelli[d], R. Lapasin[a], D. Perin[a], M. Grassi[a,*]

[a] Department of Chemical, Environmental and Raw Materials Engineering, DICAMP, University of Trieste, Piazzale Europa 1, I-34127 Trieste, Italy
[b] Department of Life Sciences, University of Trieste, Via Giorgeri 7, I-34127 Trieste, Italy
[c] Department of Clinical, Morphological and Technological Sciences, University Hospital of Cattinara, Strada di Fiume 447, I-34149 Trieste, Italy
[d] Istituto per le Applicazioni del Calcolo – CNR, Viale del Policlinico, 137, I-00161 Roma, Italy

ARTICLE INFO

Article history:
Received 4 June 2008
Accepted 7 July 2008

Keywords:
Restenosis
Mathematical modelling
Nucleic acid based drug
Gel paving

ABSTRACT

Coronary restenosis consists of the partial/total re-occlusion of the artery lumen following percutaneous transluminal angioplasty (PTCA). In order to match this pathology, PTCA is followed by the implantation of rigid scaffolds (stent or coated stent) aimed to contrast the most important mechanical (coronary wall elastic recoil and late remodelling) and biological (smooth muscle cells iper-proliferation) factors leading to restenosis. In the light of the clinical problems recently arisen about the use of traditional coated stents, this paper proposes a theoretical study to comprehend the release kinetics of novel anti-proliferative drugs, i.e. nucleic acid based drugs (NABD), complexed with the proper delivery agent (DA). The release of NABD–DA is supposed to occur from a double gel layer adhering to coronary wall and embedding the stent. The proposed mathematical model assumes that diffusion, convection and cellular internalisation/metabolism are the leading mechanisms ruling drug spreading in the coronary wall. In addition, stent void fraction, positioning (totally embedded or totally out of the coronary wall) and continuous or discontinuous character of the gel layer are other three important model parameters. In order to generalise the results, stent geometry is idealised as a series of not connected, equally spaced, rings positioned in the stented zone. In correspondence of stent strut, drug transport cannot occur.

The most important outcomes of this study are that, in the usual void fraction range (0.7–0.9), stent presence does not sensibly affect NABD–DA release kinetics. In addition, whereas stent positioning in the continuous gel configuration (totally embedded or totally out of coronary wall) is not very important, in the discontinuous case, it becomes relevant. Finally, this study evidences that a proper mixture of NABD complexed with different (in dimensions and kind) DA can ensure an almost constant NABD coronary concentration for several months, as requested by clinical observations.

1. Introduction

For many years, coronary stenosis, a common atherosclerosis complication, has been matched by means of percutaneous transluminal coronary angioplasty (PTCA), a procedure leading to the enlargement of the stenotic portion of the coronary by means of an expanding balloon. Nevertheless, the high incidence of re-stenosis (30–40%) following PTCA (Califf, 1995), obliged to consider alternative approaches. The use of stents, rigid scaffolds positioned in correspondence of the coronary vessel stenotic portion, emerged as an interesting therapeutic strategy due to the consistently reduction of re-stenosis occurrence with respect to the simple PTCA treatment (Serruys et al., 1994; Fischman et al., 1994). However, stents did not completely solve the re-stenosis problem. Although they can really prevent the coronary wall *early elastic recoil* and *late re-modelling*, two known events leading to re-stenosis, they induce *neointima* iperplasia (In Stent Restenosis – ISR) due to the iper-proliferation of vascular smooth muscle cells (VSMCs) (Ruygrok et al., 2003; Moreno et al., 2004). At this purpose, the employment of drug eluting stents releasing anti-proliferative drugs (DES) substantially reduced the VSMCs iper-proliferation and the consequent re-stenosis rate (Moses et al., 2003; Stone et al., 2004). Unfortunately, however, recent studies evidence that the re-vascularization benefit with DES is attenuated in high-risk patients (diabetes; the acute coronary syndromes; smaller-diameter lesions and longer lesions; several stents or overlapping stents), compared to low risk patients (Colombo et al., 2004). Moreover, their use is connected to a higher incidence of late thrombosis (due to an incomplete endotelisation of the stented zone) in comparison with uncoated stents (Iakovou et al., 2005). Accordingly, the necessity of undertaking new strategies arises.

* Corresponding author. Tel.: +39 040 5583435; fax: +39 040 569823.
E-mail address: mariog@dicamp.univ.trieste.it (M. Grassi).

1476-9271/$ – see front matter © 2008 Elsevier Ltd. All rights reserved.
doi:10.1016/j.compbiolchem.2008.07.013

Among the therapeutic agents that could be used, nucleic acid based drugs (NABD) have been proved to hinder VSMCs exuberant proliferation by suppressing the expression of relevant cell cycle promoting genes (Grassi et al., 2004; Khachigian et al., 2002). The fragile nature and low cellular transfection attitude impose their complexation with proper delivery agents (DA) in order to make this approach effective and reliable from the therapeutic point of view. For example, liposomes, polycations (Grassi et al., 2006) and fatty substances (Kubo et al., 2008) have been successfully considered.

The dimensions and the physico-chemical characteristics of NABD–DA complexes make their release from traditional DES problematic and alternative solutions need to be considered. The endoluminal gel paving technique (EGP) (Slepian and Hubbell, 1997), together with the implantation of a bare metal stent, seems to be an effective and promising approach. EGP consists of the catheter application of a biocompatible polymer solution on the endoluminal vessel surface followed by in situ polymerization or crosslinking. To this purpose, several catheters have been designed and their details vary according to the rheological, chemical and physical properties of polymer solutions to be inserted (Eccleston and Lincoff, 1997). In order to avoid unfavourable pressure drop across the paved zone and too high wall shear stress, gel thickness should not exceed a given threshold (typically, 300 μm with an average coronary diameter of 3 mm (Comel, 2007)). High wall shear stress can cause premature gel layer erosion. The potential advantages of the gel paving-stent technique are an easy and safe complex loading within the gel matrix and the opportunity of creating a physical barrier between the damaged coronary wall and the overflowing thrombogenic and inflammatory elements present in the blood stream (West and Hubbell, 1996). Additionally, by considering proper polymeric blends (Grassi et al., 2006; Grassi et al., 2007), it is possible the positioning of a double layers gel. While the strong part, facing blood flow prevents from premature gel erosion and limits NABD–DA complexes systemic release, the soft portion, sandwiched between coronary wall and the strong part, allows NABD–DA complexes delivery to the coronary wall where VSMCs, the target cells, reside.

Fundamental prerequisite for the success of this approach is the knowledge of NABD–DA agent complexes release kinetics to coronary wall. Accordingly, this paper is aimed to mathematical model this process in order to allow a correct system designing and to evaluate eventual peculiarities of this release system.

2. Mathematical Modelling

Let us consider an ideal drug molecule that has to spread from the lumen into the coronary wall (see Fig. 1). Firstly, it partitions in the *intima*, the innermost layer constituting coronary wall. Here, its dynamics is essentially due to diffusion, induced by the concentration gradient, and convection, due to a radial hydrostatic pressure gradient between lumen and coronary wall (Yang and Burt, 2006). In order to reach the *media* (the middle arterial wall layer), the drug molecule must partition from the *intima* to the *internal elastic lamina* and then to the *media*. Again, diffusion and convection govern its motion even though drug binding to proteins and metabolism can affect it. While drug binding to proteins is reversible, metabolism (here meant as cellular internalisation) is irreversible and leads to drug disappearing. In this context, arterial wall can be schematised as an inter-channelled structure (porous medium) where free drug molecules, moving in the fluid filling the channels, progressively bind to proteins and are metabolised (Creel et al., 2000). Again, drug molecule transport to *adventitia* (the outermost arterial wall layer) requires two further steps: *media–external elastic lamina–adventitia*. Once in the *adventitia*, the molecule is swept out by *vasa vasorum*, lymphatic drainage and lost into connective tissues. This mechanistic description of drug transport coupled with the intrinsic three-dimensional character of drug transport in the coronary wall clearly underlines the complexity of the release mechanism. Furthermore, the relative importance of the various sub-phenomena discussed (diffusion, convection, partitioning, metabolism and binding) depends on a variety of concurrent factors such as drug characteristics (molecular weight, charge, hydrophilic or hydrophobic nature), coronary structure (porosity, drug diffusion coefficient), possible wall pathological conditions and geometrical features of the release device. As a complete and detailed description of all the sub-phenomena at all scales leads to very complex models and needs the knowledge of a high number of variables and parameters (which are hardly determinable), some simplifications in modelling have been made, according to the various level of details required and the different scales involved (Prosi et al., 2005). In general, drug internalisation process is described by the following equation (Lovich and Edelman, 1996):

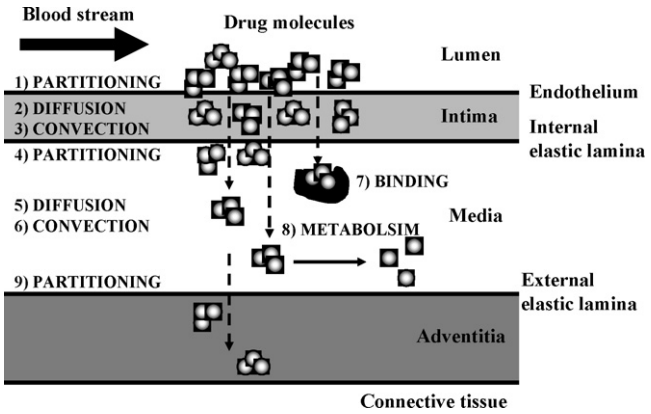

Fig. 1. Schematic representation of drug spreading inside coronary wall. The existence of both a concentration and pressure gradient between blood stream and coronary wall induces the diffusive and convective drug transport. Nevertheless, other phenomena such drug partitioning, binding and metabolism can heavily influence this transport.

$$\lambda = k_{on} B_f C + k_{off} C_b \quad (1)$$

where λ is the internalisation rate, C is the free drug concentration, C_b is the reversibly bound drug concentration, k_{on} and k_{off} are, respectively, the association and dissociation rate constants and B_f is the mole density of the active free links. Nevertheless, physiological evidences show that, once internalised inside cells, NABD–DA complexes will never come out (i.e. $k_{off} = 0$; for the sake of simplicity, we name k the product $k_{on}B_f$). In the practical impossibility of retrieving reasonable estimation of NABD–DA diffusion coefficient inside each layer, coronary wall is considered as a homogeneous medium characterised by a unique NABD–DA diffusion coefficient. In addition, despite of many possible different geometries, stent is schematised (see Fig. 2) by a series of equally spaced rings (with S_D, the inter-rings distance), characterised by axial length S_Z, radial thickness S_R and internal radius R_{is}, determining a stented zone of length Z_0. This hypothesis, jointly with the assumption of an initial uniform NABD–DA concentration in the strong and soft gel layers coating blood faced coronary wall (coronary wall is initially empty of NABD–DA), allows concluding that, due to symmetry reasons, the tangential component of the concentration gradient is zero. Finally, remembering that convective drug transport can occur only in the radial direction (the only non-zero component of the pressure gradient existing between blood stream and coronary wall is the radial one), the mass balance equation modelling drug concen-

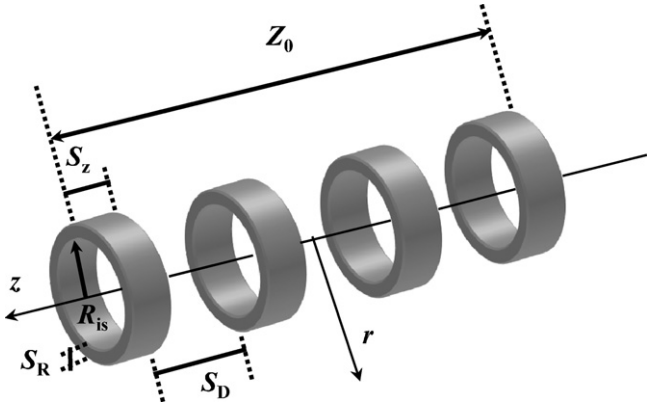

Fig. 2. Schematic representation of stent geometry. A series of equally spaced (S_D) rings, characterised by axial length S_Z, radial thickness S_R and internal radius R_{is}, constitutes the idealised stent (Z_0 represents the stented zone length; figure not in scale).

tration inside coronary wall and gel layers reads:

$$\frac{\partial C_i}{\partial t} = \frac{\partial}{\partial z}\left(\frac{\partial C_i}{\partial z}\right) + \frac{D_i}{r}\frac{\partial}{\partial r}\left(r\frac{\partial C_i}{\partial r}\right) - v_r\frac{\partial C_i}{\partial r} - kC_i \quad (2)$$

where t indicates time, r and z the radial and axial coordinates, respectively, v_r the constant radial convection (filtration) velocity (it is assumed zero in the gel layers and in all the coronary wall portions shielded by gel) while C_i and D_i are, respectively, the NABD–DA concentration and diffusion coefficient in the layer "i" ($i = cw \Rightarrow$ coronary wall, $i = stg \Rightarrow$ strong gel layer, $i = sog \Rightarrow$ soft gel layer). Aimed to a general treatment, Eq. (2) dimensionless form is considered:

$$\frac{\partial C_i^+}{\partial t} = \left(\frac{R_0}{Z_0}\right)^2\frac{\partial}{\partial z^+}\left(\frac{\partial C_i^+}{\partial z^+}\right) + \frac{1}{r^+}\frac{\partial}{\partial r^+}\left(r^+\frac{\partial C_i^+}{\partial r^+}\right) - \mathrm{Pe}\frac{\partial C_i^+}{\partial r^+} - \mathrm{Da}C_i^+ \quad (3)$$

where $C_i^+ = C_i/C_0$, $r^+ = r/R_{ecw}$, $z^+ = z/Z_0$, $t^+ = tD/R_{ecw}^2$, $\mathrm{Pe} = v_r R_{ecw}/D_{cw}$, $\mathrm{Da} = kR_{ecw}^2/D_{cw}$, R_{ecw} is the external coronary radius, C_0 is the initial concentration in the soft and strong gel layers, Pe is the Peclet number (it represents the relative importance of the convective to the diffusive effects) and Da the Damkholer number, expressing the ratio between the drug internalisation and diffusion rate (Lovich and Edelman, 1996). For simplicity, in the following, the superscript "+" will be usually omitted.

Before discussing the initial and boundary conditions required to solve Eq. (3), it is necessary defining the different configurations that can take place *in vivo* when EGP approach is adopted. The simplest situation consists in a un-stented coronary (stent absence – SA), depicted in Fig. 3a. In this case, the domain is simply given by a three-layers system constituted by strong gel, soft gel and coronary wall. Obviously, the picture complicates when stent is present. Consequently to PTCA, the atherosclerotic plaque is compressed toward the arterial wall and this leads some compenetration of the two tissues. According to the plaque composition, two limit cases are recognised: a soft material where the stent is easily inserted, or, at the other hand, a hard medium (calcified plaque) where stent insertion is hindered. Accordingly, the two limit configurations will be considered: totally embedded stent (TE) and totally out stent (TO). In addition, we account also for the possibility that the gel layer be continuous (CG) or discontinuous (DG). Indeed, especially in the case of extended paved-stented zone (>2 cm), the CG could lead to problems connected with the occlusion of secondary branches detaching from the main coronary. Fig. 3 schematically shows the

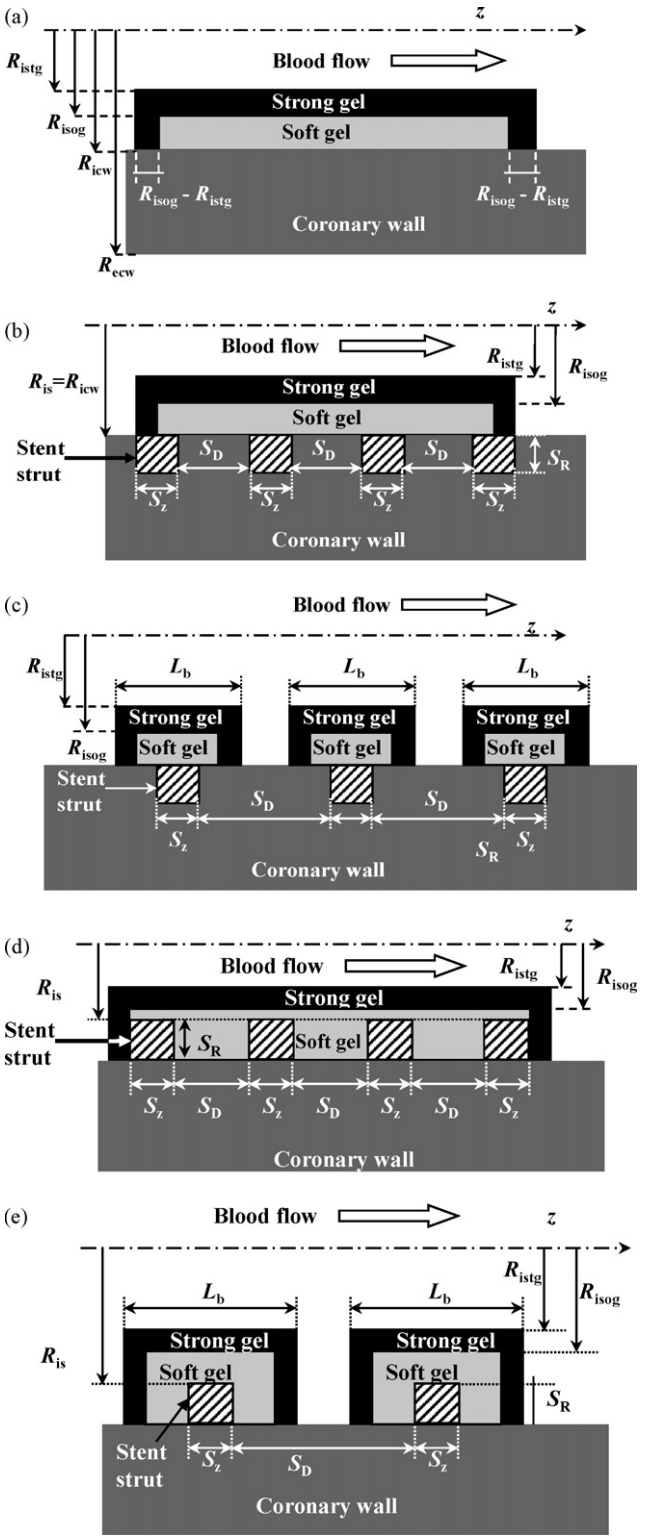

Fig. 3. Possible spatial relations among stent strut, gel layers and coronary wall (figure not in scale). The simplest situation occurs in the stent absence (SA configuration – a). In the case of soft plaque, stent can be considered totally embedded (TE) in the coronary wall while gel layers can be continuous (TE–CG configuration – b) or discontinuous (TE–DG configuration – c). When hard (calcified) plaque occurs, stent penetration in the coronary wall is hindered and the stent can be thought totally out (TO). Also in this case gel layers can be continuous (TO–CG configuration – d) or discontinuous (TO–DG configuration – e).

different configurations above described: totally embedded stent with continuous (TE–CG, Fig. 3b) or discontinuous gel (TE–DG, Fig. 3c) and totally out stent with continuous (TO–CG, Fig. 3d) or discontinuous gel (TO–DG, Fig. 3e). Although each different configuration needs to be modelled with proper boundary conditions for the solution of Eq. (3), the criteria adopted for defining boundary conditions are always the same. It is assumed that at each interface separating two phases where mass transport can occur (this is hindered in correspondence of stent strut) no mass accumulation takes place:

$$D_i \nabla C_i = D_j \nabla C_j \qquad \frac{C_i}{C_j} = k_{ij} \quad \text{at interface } i-j \tag{4}$$

where subscripts refer to generic phase i and j, respectively, and k_{ij} is the concentration independent partition coefficient. Mass flux is set to zero on all strut surfaces and on the external coronary wall (at $r = R_{ecw}$, see Fig. 3a). Axial (z-direction) mass flux at the beginning ($z = 0$) and at the end ($z = Z_0$) of the paved-stented zone is set proportional to local interface concentration:

$$D_i \left.\frac{\partial C_i}{\partial z}\right|_{z=0} = \beta C_i\,(\text{at } z = 0) \qquad D_i \left.\frac{\partial C_i}{\partial z}\right|_{z=z_0} = -\beta C_i\,(\text{at } z = z_0) \tag{5}$$

The parameter β controls the flux at inlet and at outlet, ranging from zero to infinite. In order to evaluate NABD–DA concentration dispersed in the blood and related tissues (C_b) (and, thus, at the strong gel layer-blood interface) the following global mass balance has been adopted:

$$M_0 = M_{GL}(t) + M_{CW}(t) + V_b C_b(t) + M_M(t)$$
$$C_b = k_{sb} C_{sg}(r = R_{istg}) \tag{6}$$

where M_0 is the initial NABD–DA amount present in the strong and soft gel layers (also referred to as NABD–DA dose), V_b is drug distribution volume (greater than or equal to blood volume), C_{sg} is NABD–DA concentration at the strong gel–blood interface, k_{sg} is the partition coefficient and R_{istg} is the strong gel inner radius (see Fig. 3a). M_{GL} and M_{CW} are, respectively, the NABD–DA amount present in the gel layers (strong and soft) and coronary wall at time t while M_M represents the NABD–DA amount metabolised up to t. They can be mathematically expressed by:(7)

$$M_{GL} = \int_0^{2\pi} \iint_{sog} C_{sog}(t, r, z) \mathrm{rd}\,\vartheta\,\mathrm{d}r\;\mathrm{d}z + \int_0^{2\pi} \iint_{stg} C_{stg}(t, r, z) \mathrm{rd}\,\vartheta\,\mathrm{d}r\;\mathrm{d}z$$
$$M_{CW} = \int_0^{2\pi} \iint_{cw} C_{cw}(t, r, z) \mathrm{rd}\,\vartheta\,\mathrm{d}r\,\mathrm{d}z$$
$$M_M = \int_0^{t} \int_0^{2\pi} \iint_{cw} k C_{cw}(t, r, z) \mathrm{rd}\,\vartheta\,\mathrm{d}r\,\mathrm{d}z\,\mathrm{d}t$$

In all configurations (see Fig. 3), it is supposed that initial NABD–DA concentration is uniform and equal to C_0 in both the strong and soft gel environment. On the contrary, initial NABD–DA concentration is set to zero in the coronary wall.

2.1. Model Parameter Estimation, Settings and Simulations

Eq. (3) is numerically solved adopting the control volume method (Patankar, 1980). This approach is based on the calculation domain subdivision into a number of non-overlapping control volumes (slab, cylinder, sphere, for example) where the differential equation is integrated assuming that NABD–DA concentration is constant inside each control volume (of course, other concentration profiles, such as the linear one, can be considered). The most attractive feature of this approach is that the resulting solution implies the integral conservation of quantities such as mass, momentum and energy in each control volume and, thus, in the whole calculation domain. Thus, even coarse-grid solution exhibits exact integral balances. In order to ensure numerical solution reliability, the domain has been subdivided into 6400 control volumes (rings characterised by same axial and radial thickness) in order to have 80 subdivisions in both the axial (z) and radial direction (r, 20×80 rings for the strong and soft gel layer, respectively, and 40×80 rings for the coronary wall). The linear system of equations descending from the control volume approach has been solved iteratively according to the Gauss–Seidel method adopting a relaxation factor equal to 1.6 (Chapra and Canale, 1998). Time integration (step Δt = to 3600 s) has been performed according to an implicit Euler approach.

In order to make the mathematical model and the simulations adhering to real conditions, some parameters need to be evaluated. As, usually stent struts have thickness ranging from 50 to 150 μm (Hara et al., 2006), we set $S_R = 100$ μm. In order to get averaged values for S_D and S_Z (see Fig. 2), it is worth referring to stent void fraction Φ defined as

$$\Phi = \frac{N_V S_D}{N_V S_D + N_P S_Z} \qquad N_P = N_V + 1 \tag{8}$$

where N_P is the number of rings (strut) constituting the stent, and N_V, the inter-strut voids, that equals $N_P - 1$. Accordingly, S_Z e S_D can be expressed as function of Φ:

$$S_D = Z_0 \frac{\Phi}{N_V} \qquad S_Z = Z_0 \frac{1 - \Phi}{1 + N_V} \tag{9}$$

where $Z_0 = 1.6$ cm and Φ is usually ≥80% (Chen and Liang, 2005). Stent internal radius, R_{is}, is set equal to coronary internal radius $R_{icw} = 0.15$ cm while coronary external radius, R_{ecw}, is set equal to 0.25 cm (Guyton and Hall, 2007). As thick paving layers would cause unacceptable pressure drop across the paved zone and too high wall shear stress, strong and soft gel layer thickness are set equal to 20 and 220 μm, respectively (Comel, 2007). According to literature suggestion (Yang and Burt, 2006), the radial convective velocity v_r is set equal to 1.3×10^{-8} cm/s in the coronary wall portion ($R_{ecw} < r < R_{icw}$) facing the blood stream. On the other way around, $v_r = 0$ where the coronary wall is shielded by the gel layer or by the stent strut from a direct contact with blood stream.

As NABD–DA diffusion coefficient in the coronary wall strongly depends on delivery agent nature, in the light of their large use in this field, we considered liposomes as DA. In particular, reference is made to experimental results coming from the work of Khachigian and co-workers (Santiago et al., 1999). On this basis, the NABD–DA diffusion coefficient in the coronary wall (D_{cw}) can be estimated equal to 10^{-12} cm^2/s (Davia, 2006). As, again, NABD–DA diffusion coefficient in the soft gel layer strongly depends on gel properties (such as polymer concentration and crosslinking degree) and on NABD–DA dimensions, we refer to the work of Grassi and co-workers (Grassi et al., 2007) who considered liposomes as delivery agent and a soft gel layer made up by pluronic/alginate blend (gelation due to temperature). Accordingly, NABD–DA diffusion coefficient in the soft gel layer (D_{sog}) reveals to be of the order of 10^{-11} cm^2/s. With reference to the same experimental frame, NABD–DA diffusion coefficient in the strong gel layer (D_{stg}) has been set 10^{-14} cm^2/s. Although very rough, this estimation simply remembers that NABD–DA diffusion coefficient in the strong gel layer should vanish due to the small dimension of gel mesh. Resorting to the paper of Lovich and Edelman (1996), the internalisation constant (k) order of magnitude has been set equal to 10^{-5} s^{-1}, while distribution volume V_b has been set equal to 8000 cm^3 (Davia,

2006). Finally, we set $\beta = D_{cw}/\Delta z = 5 \times 10^{-11}$ cm/s, where Δz indicates the step length in the axial (z) direction.

3. Results and Discussion

In order to better understand model features, it is convenient to separately analyze the effects of the many parameters that can, potentially, rule NABD–DA delivery in the coronary wall. First of all, internalisation and diffusive properties will be studied. Then, an idealised stent geometry and configuration will be considered and delivery system optimisation will be proposed in such a case. In all the following model simulations, it is implicitly assumed that gel layer undergoes neither swelling nor significant erosion due to blood stream action and/or enzymatic/metabolic activity.

3.1. Internalisation—Diffusion

We firstly examine pure drug diffusion in the case of stent absence (Fig. 3a). Accordingly, we fix Pe = 0 and $D_{stg}/D_{cw} = 0.01$, while the ratio D_{sog}/D_{cw} and the Damkholer number are varied. All other parameters have been set as in Section 2.1. Assuming $D_{sog}/D_{cw} = 10$, Fig. 4 shows that the NABD–DA dimensionless average coronary wall concentration C_{cw} reduces with Da, i.e. with the drug internalisation parameter, whatever the dimensionless time considered. As a matter of fact, for increasing Da, the drug mass that is internalised by cells – and is no longer free to diffuse – grows. It has been observed that the drug amount internalised at the end of simulation increases as log (Da). If, on the other hand Da = 0, the NABD–DA concentration in the wall decreases for increasing values of D_{sog}/D_{cw} (see Fig. 5). On the opposite side, an increase of D_{sog}/D_{cw} accelerates the NABD–DA loss in the blood. When $D_{sog}/D_{cw} \geq 10^3$, almost all NABD–DA disperses in the blood. The above considerations make clear that NABD–DA delivery in the coronary wall is extremely dependent on internalisation (here represented by Da) and diffusion ratio (D_{sog}/D_{cw}).

3.2. Stent Geometry and Depth

This analysis basically subdivides into two different situations: (*a*) the gel layer continuously coats the coronary inner wall (Fig. 3b and d) (*b*) gel coating is discontinuous (Fig. 3c and e).

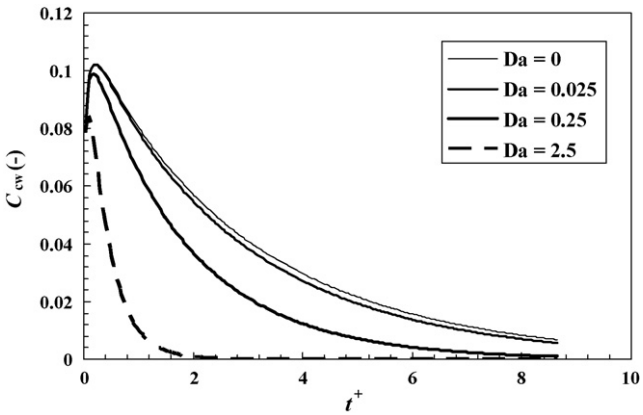

Fig. 4. NABD–DA dimensionless average coronary wall concentration C_{cw} versus dimensionless time t^+ assuming different Damkholer number (Da) values, fixing $D_{sog}/D_{cw} = 10$, $D_{stg}/D_{cw} = 0.01$ and Pe = 0 (inside coronary wall) (continuous gel configuration in the stent absence. See Fig. 3a).

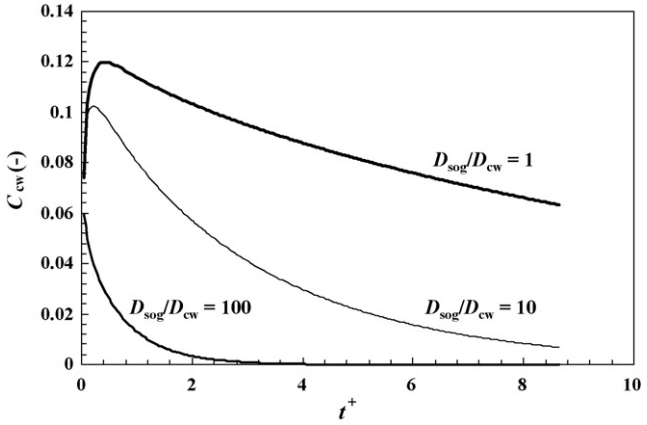

Fig. 5. NABD–DA dimensionless average coronary wall concentration C_{cw} versus dimensionless time t^+ assuming different values for the ratio D_{sog}/D_{cw}, fixing $D_{stg}/D_{cw} = 0.01$ and Da = Pe = 0 (inside coronary wall) (continuous gel configuration in the stent absence. See Fig. 3a).

3.2.1. Continuous Gel Layer

In order to evaluate the effect of stent geometry on C_{cw}, we considered a totally embedded stent configuration (see Fig. 3b) with Da = 0, Pe = 0, $D_{stg}/D_{cw} = 0.01$, $D_{sog}/D_{cw} = 10$ and different ϕ_V (0.7, 0.8, 0.9) and N_V (6, 9, 12) values. Accordingly, nine different systems have been simulated. Simulation results (data not shown) make clear that, whatever N_V, stent void fraction (ϕ_V) variation in the proposed range (0.7–0.9) does not play a very significant role in the C_{cw} time profile. The concentration surface $C_{cw}(z^+, r^+)$ in the gel/wall system correspondent to half-stent at time $t^+ = 0.025$ with $\phi_V = 0.7$ and $N_V = 6$, is depicted in Fig. 6. Note the two concentration gradients components driving drug diffusion: the first, directed towards to the arterial wall, and the second one in the opposite direction (blood stream). Moreover, we can observe some concentration peaks where stent struts hinder drug dynamics. This 3D picture further confirms that, in the usual ϕ_V range ($\geq$0.7) (Chen and Liang, 2005), the hindering action exerted by the stent on NABD–DA delivery to the coronary wall is limited. In addition it can be seen

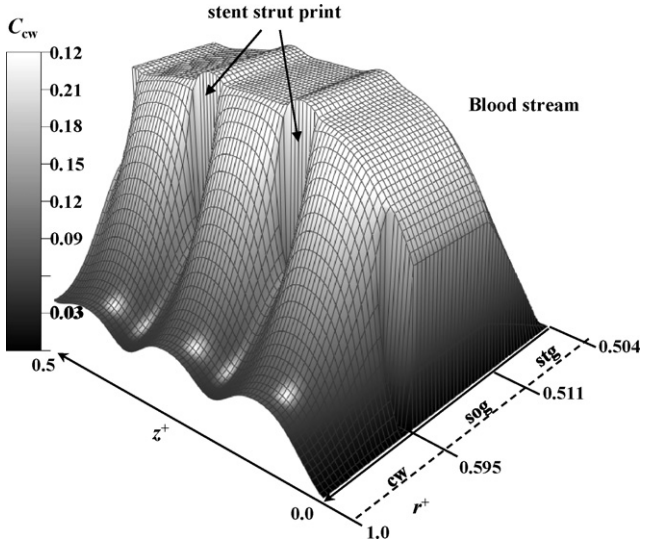

Fig. 6. NABD–DA dimensionless coronary wall concentration C_{cw} versus the dimensionless radial (r^+) and axial (z^+) co-ordinates assuming Da = 0, Pe = 0, $D_{stg}/D_{cw} = 0.01$, $D_{sog}/D_{cw} = 10$, $\phi_V = 0.7$, $N_V = 6$ and $t^+ = 0.025$ (continuous gel configuration with totally embedded stent. See Fig. 3b). "*cw*", "*sog*" and "*stg*" indicate the simulation field competing to coronary wall, soft and strong gel layer, respectively (figure not in scale). Dark intensity in the vertical left bar is proportional to NABD–DA concentration.

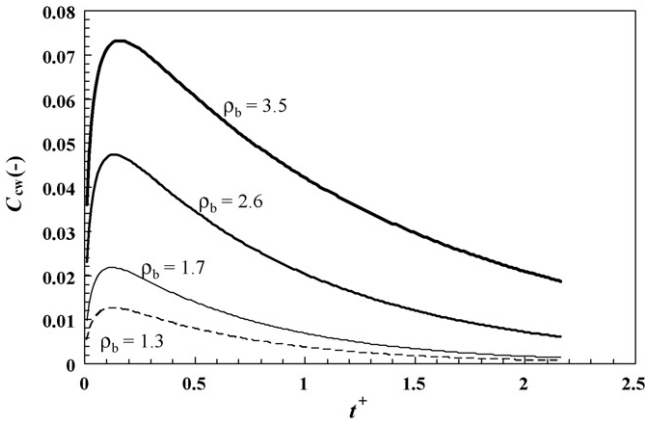

Fig. 7. Effect of ρ_b (ratio between the band width L_b and the strut axial width S_Z. Discontinuous gel configuration and totally embedded stent. See Fig. 3c) on the temporary trend of the NABD–DA dimensionless average coronary wall concentration C_{cw} assuming $\phi_V = 0.8$, $N_V = 6$, $S_R = 0.01$ cm, $D_{stg}/D_{cw} = 0.01$, $D_{sog}/D_{cw} = 10$ and Da = 0. Pe = 0 in correspondence of gel bands, while Pe = 10 elsewhere.

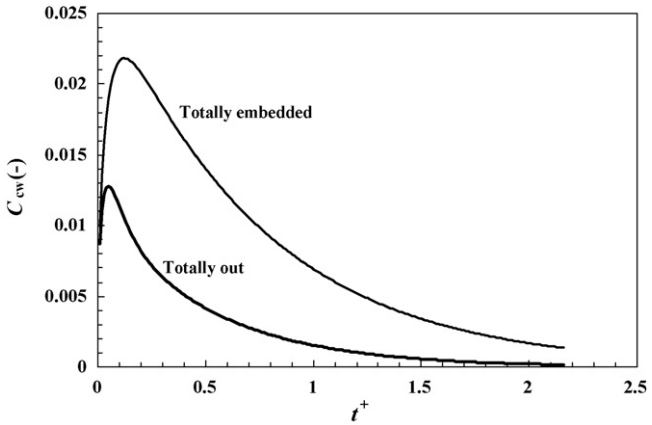

Fig. 8. Comparison between the totally out and totally embedded stent dispositions (discontinuous gel configuration. See Fig. 3c–e TO) assuming $\rho_b = 1.7$ and the same parameters values considered in Fig. 7. C_{cw} is the NABD–DA dimensionless average coronary wall concentration.

that NABD–DA concentration rapidly decreases with radial position once the soft gel layer is overcame. This means that NABD–DA mainly lies where its therapeutic action is needed, i.e. around the soft gel/coronary wall interface. Indeed, we do not want to hinder the proliferation of inner cells. Of course, this situation is due to the particular values adopted for D_{stg}/D_{cw} and D_{sog}/D_{cw}.

Assuming the same parameters adopted in the totally embedded configuration, we simulated another system where the stent is totally out of the artery, and fully incorporated in the gel (Fig. 3d). Analysis of the influence of ϕ_V and N_V provides identical results: the hindrance to drug release undergoes approximately the same characteristics than the totally embedded case.

3.2.2. Discontinuous Gel Layer

Let us now examine the case where the gel is only spread over a single strut, resulting in a series of circular rings separated by areas where coronary wall is in direct contact with blood. In such a case, it is not possible setting Pe = 0 uniformly, as gel layer no longer shields all the coronary inner surface competing to the stented zone. Accordingly, in order to stress its effect, we set a high Pe (=10) for the volumes where the coronary wall is in contact with blood flow. In all the other volumes, we set Pe = 0. In this configuration, the effect of ρ_b, defined as the ratio between the band width L_b and the strut axial width S_Z (see Fig. 3c) is considered. The influence of this parameter was studied in the two limit configurations previously considered (totally out and totally embedded stent). The geometry of the stent is fixed as $(\phi_V; N_V; S_R) = (0.8; 6; 0.01\text{ cm})$ while $D_{stg}/D_{cw} = 0.01$ and $D_{sog}/D_{cw} = 10$. In order to investigate the effect of the only ρ_b parameter, the internalisation constant k is set to zero (Da = 0). In the totally embedded configuration, strong and soft gel layer are, respectively, 20 and 200 μm thick. Fig. 7 shows that the average drug concentration in the coronary wall grows with ρ_b, as not only the gel/coronary wall interface increases with ρ_b but also the gel volume and, thus, the NABD–DA dose, increases with ρ_b.

While, qualitatively, the effect of ρ_b on NABD–DA delivery from totally out stent is the same, differences among the two configurations (TO and TE) arise from a quantitative point of view. In Fig. 8, a comparison between the TO and TE configurations is shown ($\rho_b = 1.7$): in the former case the concentration profile is relatively lower. This is due to the fact that the stent fills a larger volume of gel layer, this resulting in a lower amount of deliverable drug. Interestingly, while in the continuous configuration drug release is not influenced by the stent penetration depth, in the present case the profiles exhibit a remarkable difference: in the totally out stent the average concentration is approximately halved with respect to the embedded stent.

3.3. System Optimisation

Once the effects and the sensitivity to the model parameters have been studied, it is worth running a simulation about a possible realistic situation. Model parameters have been set according to what discussed in Section 2.1: stent length $Z_0 = 1.6$ cm, stent internal radius R_{is}, = 0.15 cm; strong gel layer thickness = 20 μm; soft gel layer thickness = 200 μm; external coronary radius $R_{ecw} = 0.25$ cm; internal coronary radius $R_{icw} = 0.15$ cm; stent void fraction $\Phi_V = 0.8$, inter-strut spaces $N_V = 6$, diffusion coefficient in the strong gel layer $D_{stg} = 10^{-14}$ cm^2/s, diffusion coefficient in the soft gel layer $D_{sog} = 10^{-11}$ cm^2/s, diffusion coefficient in coronary wall $D_{cw} = 10^{-12}$ cm^2/s, stent thickness $S_R = 100$ μm, radial convective velocity $v_r = 1.3 \times 10^{-8}$ cm/s, internalisation constant $k = 0$. The choice of setting k to zero descends from the uncertainty of this value when liposome constitutes the delivery agent.

Fig. 9 shows the comparison between the temporary trend of NABD–DA dimensionless coronary wall average concentration C_{cw}

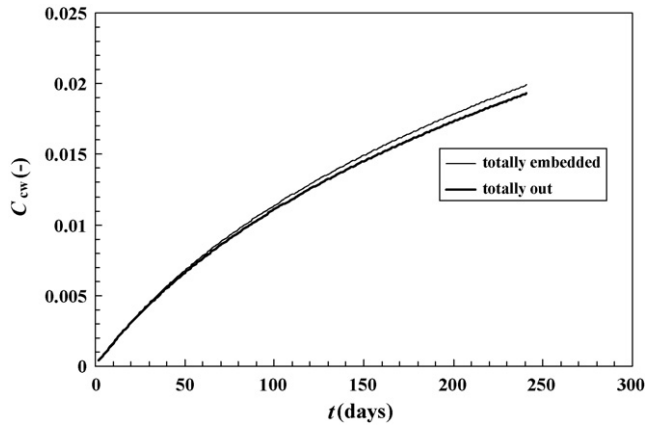

Fig. 9. Comparison between the evolution of NABD–DA coronary wall average concentration C_{cw} in the case of totally embedded and totally out stent configuration (continuous gel layer. See Fig. 3b–d) (stent length $Z_0 = 1.6$ cm, $R_{is} = 0.15$ cm, strong gel layer thickness = 20 μm, soft gel layer thickness = 200 μm, $R_{ecw} = 0.25$ cm, $R_{icw} = 0.15$ cm, $\Phi_V = 0.8$, $N_v = 6$, $D_{stg} = 10^{-14}$ cm^2/s, $D_{sog} = 10^{-11}$ cm^2/s, $D_{cw} = 10^{-12}$ cm^2/s, $S_R = 100$ μm, $v_r = 1.3 \times 10^{-8}$ cm/s, $k = 0$).

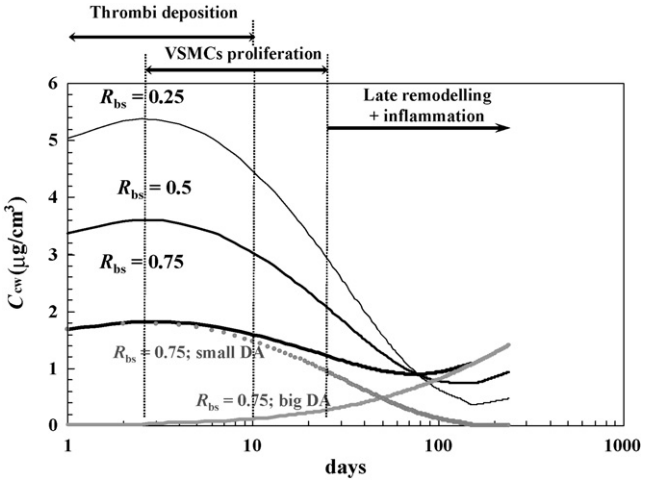

Fig. 10. Comparison among some patho-biological events (*thrombi deposition*, *VSMCs proliferation*, *late remodelling and inflammation*) following stent implantation and simulated temporary evolution (lines) of mean coronary wall NABD–DA concentration (C_{cw}) assuming three different initial conditions. In the first case, the ratio between the gel layers concentration of NABD complexes carrying big and small delivery agents is R_{bs} = 0.5 (thin line), while it is R_{bs} = 0.5 (medium line) and 0.75 (thick line) in the other two cases. In particular, dotted and solid grey curves indicate, respectively, the contribution to the overall concentration (C_{cw}) of NABD complexes carrying small and big delivery agents in the case R_{bs} = 0.75 (all other simulation parameters are those set in Fig. 9).

in the case of totally embedded (upper curve) and totally out (lower curve) stent configuration (continuous gel layer). It can be noticed that, irrespective of the stent configuration, C_{cw} approximately reaches 1.5% C_0 only after 3.5 months from stent implantation and no significant differences arise between the two configurations. It is interesting noticing that, due to the extremely low diffusion coefficient in the strong gel layer, NABD–DA systemic release is, after 1 year, only the 3% of the drug amount initially loaded in the gel layers (drug dose).

The extreme low C_{cw} increase shown in Fig. 9 makes clear that the delivery system needs to be improved in order to make it effective and reliable. Indeed, NABD–DA release kinetics results too slow in comparison with some peculiar phenomena leading to neointimal development. Typically, platelet-rich thrombi deposition and monocyte adherence on the stented zone develop in about 10 days while VSMCs and monocytes proliferation start after 2–3 days and last, approximately, for the successive 30–40 days (see Fig. 10). On the other hand, late coronary remodelling and inflammation are clearly evident after 20–30 days (Edelman and Rogers, 1998). Accordingly, what we need is a two steps release able to hinder both fast and slow restenotic events. This target can be reached considering delivery agents characterised by different diffusivity. If liposomes, in virtue of their large size (~700 nm) can guarantee a small NABD–DA diffusivity, smaller delivery agents such as cholesterol or polycations ensure much higher NABD–DA mobility. Accordingly, it has been simulated a gel layer containing NABD bound with big delivery agents (such liposomes) or small delivery agents (such cholesterol). It has been assumed that small delivery agents confer to NABD–DA $D_{cw} = 10^{-8}$ cm^2/s, $D_{sog} = 10^{-7}$ cm^2/s and $D_{stg} = 10^{-10}$ cm^2/s. These values have been estimated assuming that DA does not sensibly alter NABD motion so that they should represent NABD diffusion coefficient in the gel layers and in the coronary wall. In addition, due to the low whole initial NABD–DA concentration in the gel layers (C_0 = 70 μg/cm^3 (Grassi et al., 2005) the diffusive NABD–DA processes, competing to large and small size DA, do not reciprocally influence. Accordingly, their diffusion coefficients depend on zone (coronary wall, strong and soft gel layer) and NABD–DA characteristics. Fig. 10 shows the temporary trend of mean coronary wall NABD–DA concentration (C_{cw}) assuming three different initial conditions. In the first case (upper curve), the initial gel concentration of NABD complexes with big and small DA is C_{ib} = 17.5 and C_{is} = 52.5 μg/cm^3, respectively (ratio $R_{bs} = C_{ib}/(C_{ib} + C_{is}) = 0.25$). In the second case, we have C_{ib} = 35 and C_{is} = 35 μg/cm^3, respectively (ratio R_{bs} = 0.5) and in the third case we have C_{ib} = 52.5 and C_{is} = 17.5 μg/cm^3, respectively (ratio R_{bs} = 0.75). In each case, it is evident that small DA mainly determines NABD–DA concentration in the first 30 days while big DA is responsible for NABD–DA concentration in the following months. Accordingly, thrombi deposition, monocyte and VSMCs proliferation should be hindered by NABD–DA complexes containing small DA, while late coronary remodelling and inflammation should be matched by NABD–DA complexes containing large sized DA. It is worth noting that, a proper modulation of the ratio R_{bs} allows exalting or depressing the amplitude of the fast and late NABD–DA action. In particular, in the R_{bs} = 0.75 case, an almost constant temporary concentration is realised in the simulated 8 months. Finally, Fig. 10, relatively to the R_{bs} = 0.75 case, reports the C_{cw} evolution relatively to small (grey dotted curve) and large sized DA complexes (grey continuous curve).

4. Conclusions

The performed simulations reveal that drug spreading inside the coronary wall and in the blood stream strongly depends on the internalisation rate (accounted by the Damkholer number Da) and on the ratio between NABD–DA diffusion coefficient in the coronary wall and in the soft gel layer (D_{cw}/D_{sog}) provided that the NABD–DA diffusion coefficient in the strong gel layer is small in comparison with that of the soft gel layer (≤0.1%). In particular, the amount of internalised NABD–DA increases with the logarithm of Da. Despite the presence of the strong gel layer, when $D_{sog}/D_{cw} > 10^3$, the complex majority is lost in the blood stream due to the huge diffusive resistance exerted by the coronary wall. Interestingly, when liposome is the carrier, our simulations indicate that NABD tends to remain near the coronary wall/soft gel interface where the therapeutic action needs to be exploited. In the usual void fraction range ($0.7 \le \phi_V \le 0.9$), the effect of stent depth (totally out or totally in) does not sensibly affect release kinetics if the continuous gel layer configuration is considered. On the contrary, in the discontinuous configuration, stent position is deemed important. Indeed, being fixed gel layer thickness, stent presence reduces gel volume devoted to host the NABD–DA complex (decreased available dose).

Finally, our simulations suggest that by properly playing on NABD diffusivity (acting on the carrier dimensions) it is possible modulating NABD release kinetics in order to match the requirements dictated by the cascade events leading to restenosis. In particular, adopting a mixture of small and big carriers (ratio 0.75:0.25), it is possible maintaining an almost constant mean coronary NABD concentration over a period of several months.

Acknowledgments

This work was in part supported by the “Fondazione Cassa di Risparmio of Trieste”, by the “Fondazione Benefica Kathleen Foreman Casali of Trieste” and by “Fondo Trieste 2006”. Authors are very grateful to Dr. Andrea Perkan (S. C. Cardiologia Az. Ospeadali Riuniti, Trieste, Italy) for helpful discussions.

References

Califf, R.M., 1995. Restenosis: the cost to society. Am. Heart J. 130, 680–684.
Chapra, S.C., Canale, R.P., 1998. Numerical Methods for Engineers, 3rd ed. McGraw-Hill, Boston (chapter 11).

Chen, M.C., Liang, H.F., 2005. A novel drug-eluting stent spray-coated with multilayers of collagen and sirolimus. J. Control. Release 108, 178–188.
Colombo, A., Moses, J.W., Morice, M.C., Ludwig, J., Holmes Jr., D.R., Spanos, V., Louvard, Y., Desmedt, B., Di Mario, C., Leon, M.B., 2004. Randomized study to evaluate sirolimus-eluting stents implanted at coronary bifurcation lesions. Circulation 109, 1244–1249.
Comel, L., 2007. Aspetti fluidodinamici connessi alla restenosi coronarica. Graduate thesis, Department of Materials Engineering, Trieste University, Italy.
Creel, C., Lovich, M., Edelman, E., 2000. Arterial paclitaxel distribution and deposition. Circ. Res. 86 (8), 879–884.
Davia, L., 2006. Simulazione del processo di rilascio da uno stent medicato. Graduate thesis, Department of Chemical Engineering, Trieste University, Italy.
Eccleston, D.S., Lincoff, A.M., 1997. Catheter-based delivery for restenosis. Adv. Drug Deliv. Rev. 24, 31–43.
Edelman, E.R., Rogers, C., 1998. Pathobiologic responses to stenting. Am. J. Cardiol. 81, 4E–6E.
Fischman, D.L., Leon, M.B., Baim, D.S., Schatz, R.A., Savage, M.P., Penn, I., Detre, K., Veltri, L., Ricci, D., Nobuyoshi, M., 1994. A randomized comparison of coronary-stent placement and balloon angioplasty in the treatment of coronary artery disease. Stent Restenosis Study Investigators. N. Engl. J. Med. 331, 496–501.
Grassi, G., Crevatin, A., Farra, R., Guarnieri, G., Pascotto, A., Rehimers, B., Lapasin, R., Grassi, M., 2006. Rheological properties of aqueous pluronic-alginate systems containing liposomes. J. Colloid Interface Sci. 301, 282–290.
Grassi, G., Dawson, P., Guarnieri, G., Kandolf, R., Grassi, M., 2004. Therapeutic potential of hammerhead ribozymes in the treatment of hyper-proliferative diseases. Curr. Pharm. Biotechnol. 5 (4), 369–386.
Grassi, G., Farra, R., Noro, E., Voinovich, D., Lapasin, R., Dapas, B., Alpar, O., Zennaro, C., Carraro, M., Giansante, C., Guarnieri, G., Pascotto, A., Rehimers, B., Grassi, M., 2007. Characterisation of nucleid acid molecule/liposome complexes and rheological effects on pluronic/alginate matrice. J. Drug Deliv. Sci. Technol. 17 (5), 325–331.
Grassi, G., Farra, R., Caliceti, P., Guarnieri, G., Carenza, M., Grassi, M., 2005. Temperature-sensitive hydrogels: potential therapeutic applications. Am. J. Drug Del. 3, 239–251.
Guyton, A.C., Hall, J.E., 2007. Textbook of Medical Physiology. Elsevier Saunders.
Hara, H., Nakanura, M., Palmaz, J.C., Schwartz, R.S., 2006. Role of stent design and coatings on restenosis and thrombosis. Adv. Drug Deliv. Rev. 58, 377–386.
Iakovou, I., Schmidt, T., Bonizzoni, E., Ge, L., Sangiorgi, G.M., Stankovic, G., Airoldi, F., Chieffo, A., Montorfano, M., Carlino, M., Michev, I., Corvaja, N., Briguori, C., Gerckens, U., Grube, E., Colombo, A., 2005. Incidence, predictors, and outcome of thrombosis after successful implantation of drug-eluting stents. JAMA 293, 2126–2130.
Khachigian, L.M., Fahmy, R.G., Zhang, G., Bobryshev, Y.V., Kaniaros, A., 2002. c-Jun regulates vascular smooth muscle cell growth and neointima formation after arterial injury. Inhibition by a novel DNA enzyme targeting c-Jun. J. Biol. Chem. 277, 22985–22991.
Kubo, T., Zhelev, Z., Ohba, H., Bakalova, R., 2008. Chemically modified symmetric and asymmetric duplex RNAs: an enhanced stability to nuclease degradation and gene silencing effect. Biochem. Biophys. Res. Commun. 365 (1), 54–61.
Lovich, M.A., Edelman, E.R., 1996. Computational simulations of local vascular heparin deposition and distribution. Am. J. Physiol. 271, H2014–H2024.
Moreno, R., Fernandez, C., Alfonso, F., Hernandez, R., Perez-Vizcayno, M.J., Escaned, J., Sabate, M., Banuelos, C., Angiolillo, D.J., Azcona, L., Macaya, C., 2004. Coronary stenting versus balloon angioplasty in small vessels: a meta-analysis from 11 randomized studies. J. Am. Coll. Cardiol. 43, 1964–1972.
Moses, J.W., Leon, M.B., Popma, J.J., Fitzgerald, P.J., Holmes, D.R., O'Shaughnessy, C., Caputo, R.P., Kereiakes, D.J., Williams, D.O., Teirstein, P.S., Jaeger, J.L., Kuntz, R.E., 2003. Sirolimus-eluting stents versus standard stents in patients with stenosis in a native coronary artery. N. Engl. J. Med. 349, 1315–1323.
Patankar, S.V., 1980. Numerical Heat Transfer and Fluid Flow. Hemisphere Publishing, New York.
Prosi, M., Zunino, P., Perktold, K., Quarteroni, A., 2005. Mathematical and numerical models for transfer of low-density lipoproteins through the arterial walls: a new methodology for the model set up with applications o the study of disturbed lumenal flow. J. Biomech. 38, 903–917.
Ruygrok, P.N., Webster, M.W., Ardill, J.J., Chan, C.C., Mak, K.H., Meredith, I.T., Stewart, J.T., Ormiston, J.A., Price, S., 2003. Vessel caliber and restenosis: a prospective clinical and angiographic study of NIR stent deployment in small and large coronary arteries in the same patient. Catheter Cardiovasc. Interv. 59, 165–171.
Santiago, F.S., Lowe, H.C., Kavurma, M.M., Chesterman, C.N., Baker, A., Atkins, D.G., Khachigian, L.M., 1999. New DNA enzyme targeting Egr-1 mRNA inhibits vascular smooth muscle proliferation and regrowth after injury. Nat. Med., 1264–1269.
Serruys, P.W., de Jaegere, P., Kiemeneij, F., Macaya, C., Rutsch, W., Heyndrickx, G., Emanuelsson, H., Marco, J., Legrand, V., Materne, P., 1994. A comparison of balloon-expandable-stent implantation with balloon angioplasty in patients with coronary artery disease. Benestent Study Group. N. Engl. J. Med. 331, 489–495.
Slepian, M.J., Hubbell, J.A., 1997. Polymeric endoluminal gel paving: hydrogel sytems for local barrier creation and site-specific drug delivery. Adv. Drug Deliv. Rev. 24, 11–30.
Stone, G.W., Ellis, S.G., Cox, D.A., Hermiller, J., O'Shaughnessy, C., Mann, J.T., Turco, M., Caputo, R., Bergin, P., Greenberg, J., Popma, J.J., Russell, M.E., 2004. A polymer-based, paclitaxel-eluting stent in patients with coronary artery disease. N. Engl. J. Med. 350, 221–231.
West, J.L., Hubbell, J.A., 1996. Separation of the arterial wall from blood contact using hydrogel barriers reduces intimal thickening after balloon injury in the rat: the roles of medial and luminal factors in arterial healing. Proc. Natl. Acad. Sci. U.S.A. 93, 13188–13193.
Yang, C., Burt, H.M., 2006. Drug-eluting stents: factors governing local pharmacokinetics. Adv. Drug Deliv. Rev. 58, 402–411.